

RAB23 Mutations in Carpenter Syndrome Imply an Unexpected Role for Hedgehog Signaling in Cranial-Suture Development and Obesity

Dagan Jenkins, Dominik Seelow, Fernanda S. Jehee, Chad A. Perlyn, Luís G. Alonso, Daniela F. Bueno, Dian Donnai, Dragana Josifova, Irene M. J. Mathijssen, Jenny E. V. Morton, Karen Helene Ørstavik, Elizabeth Sweeney, Steven A. Wall, Jeffrey L. Marsh, Peter Nürnberg, Maria Rita Passos-Bueno, and Andrew O. M. Wilkie

Carpenter syndrome is a pleiotropic disorder with autosomal recessive inheritance, the cardinal features of which include craniosynostosis, polysyndactyly, obesity, and cardiac defects. Using homozygosity mapping, we found linkage to chromosome 6p12.1-q12 and, in 15 independent families, identified five different mutations (four truncating and one missense) in *RAB23*, which encodes a member of the RAB guanosine triphosphatase (GTPase) family of vesicle transport proteins and acts as a negative regulator of hedgehog (HH) signaling. In 10 patients, the disease was caused by homozygosity for the same nonsense mutation, L145X, that resides on a common haplotype, indicative of a founder effect in patients of northern European descent. Surprisingly, nonsense mutations of *Rab23* in *open brain* mice cause recessive embryonic lethality with neural-tube defects, suggesting a species difference in the requirement for RAB23 during early development. The discovery of *RAB23* mutations in patients with Carpenter syndrome implicates HH signaling in cranial-suture biogenesis—an unexpected finding, given that craniosynostosis is not usually associated with mutations of other HH-pathway components—and provides a new molecular target for studies of obesity.

Carpenter syndrome (MIM 201000), also known as “acrocephalopolysyndactyly type II,” is a rare autosomal recessive disorder characterized by craniosynostosis, obesity, polydactyly, and soft-tissue syndactyly (fig. 1).^{1–3} Unlike other inherited craniosynostoses, which most commonly affect the coronal sutures, fusion of the midline (metopic and sagittal) sutures is typical in Carpenter syndrome; severe cases have cloverleaf skull. Other well-recognized features include brachydactyly with shortening or absence of the middle phalanges, molar agenesis, genu valgum, hypogenitalism, congenital cardiac defects, umbilical hernia, and learning disability.^{3–5} Although the molecular basis of many craniosynostosis syndromes is now well described, with mutations of fibroblast growth-factor receptors, ephrins, or the transcription factor TWIST most frequently identified,⁶ the etiology of Carpenter syndrome has been elusive.

We mapped the disease locus, using a large family (family 1; subjects 3541, 3589, and 3593) from the United States.⁷ After approval from the Oxfordshire Research Ethics Committee and the local institutional review board,

DNA was collected with informed consent from six siblings (three affected and three unaffected) and both parents. The parents were not known to be related, but, of their eight grandparents, three of the father’s and two of the mother’s had been born in the same city, raising the possibility of a distant consanguineous loop. We also analyzed an affected male (family 2; subject 3624) whose Danish parents were first cousins; in addition to the classic features of Carpenter syndrome, subject 3624 had a lumbar myelomeningocele. Using the GeneChip Human Mapping 50K Array Hind240 (Affymetrix), we undertook genome-wide SNP genotyping and performed parametric multipoint linkage analysis, allowing for heterogeneity, using GENEHUNTER-MODSCORE software.⁸ In the absence of consanguinity in family 1, no significant linkage was obtained (the maximum possible heterogeneity LOD [HLOD] score of 2.7 was found for three different regions of the genome); however, when a consanguineous loop (conservatively assigned as second-cousin parents) was introduced, the HLOD score increased dramatically for just one of these regions, to a maximum of 4.8, for families 1 and

From the Weatherall Institute of Molecular Medicine, University of Oxford (D.J.; A.O.M.W.), and Craniofacial Unit, Oxford Radcliffe Hospitals National Health Service Trust (S.A.W.; A.O.M.W.), Oxford, United Kingdom; Cologne Center for Genomics and Institute for Genetics, University of Cologne, Cologne (D.S.; P.N.); Centro de Estudos do Genoma Humano, Departamento de Biologia, Universidade de São Paulo (F.S.J.; M.R.P.-B.), and Departamento de Morfologia, Universidade Federal de São Paulo (L.G.A.) and SOBRAPAR, Universidade de Campinas (D.F.B.), São Paulo; Division of Plastic Surgery, Washington University School of Medicine (C.A.P.), and Cleft Lip/Palate and Craniofacial Deformities Center, St. John’s Mercy Medical Center (J.L.M.), St. Louis; Academic Unit of Medical Genetics, University of Manchester, St Mary’s Hospital, Manchester, United Kingdom (D.D.); Clinical Genetics, Guy’s Hospital, London (D.J.); Department of Plastic and Reconstructive Surgery, Erasmus Medical Center, Rotterdam (I.M.J.M.); West Midlands Regional Genetics Service, Birmingham Women’s Hospital, Birmingham, United Kingdom (J.E.V.M.); Department of Medical Genetics, Rikshospitalet-Radiumhospitalet Medical Centre, and Faculty Division Rikshospitalet, University of Oslo, Oslo (K.H.Ø.); and Merseyside & Cheshire Clinical Genetics Service, Liverpool Women’s Hospital, Liverpool (E.S.)

Received January 16, 2007; accepted for publication March 8, 2007; electronically published April 18, 2007.

Address for correspondence and reprints: Dr. A. O. M. Wilkie, Weatherall Institute of Molecular Medicine, University of Oxford, John Radcliffe Hospital, Oxford OX3 9DS, United Kingdom. E-mail: awilkie@hammer.imm.ox.ac.uk

Am. J. Hum. Genet. 2007;80:1162–1170. © 2007 by The American Society of Human Genetics. All rights reserved. 0002-9297/2007/8006-0015\$15.00
DOI: 10.1086/518047

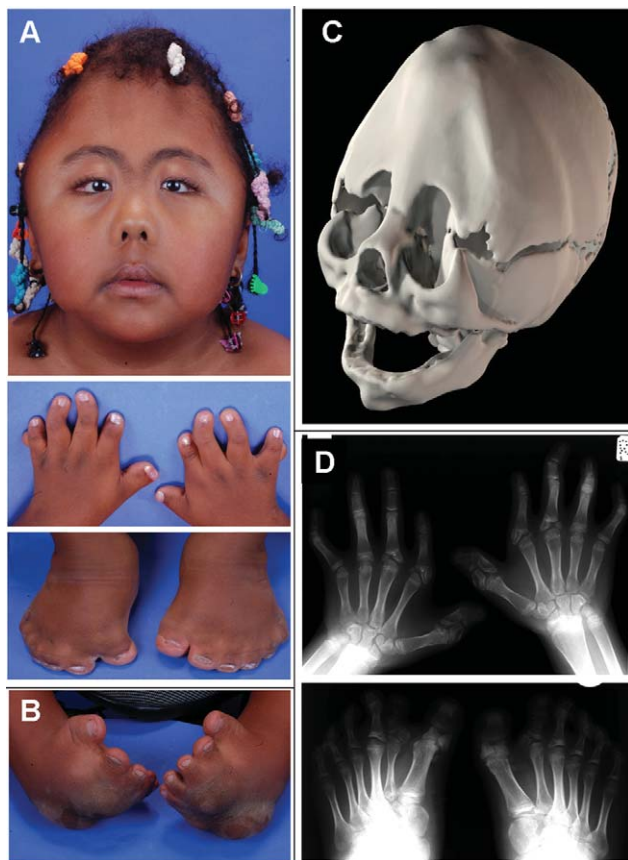


Figure 1. Clinical features of Carpenter syndrome. *A*, Affected sister of subject 4009, aged 6 years. Note metopic ridge and temporal bulging secondary to multisuture synostosis, arched eyebrows, epicanthic folds, anteverted nares, and broad thumbs and halluces with syndactyly, brachydactyly, clinodactyly, and polydactyly (postaxial in hands, central in feet). *B*, Severe bilateral clubfoot in subject 4009. *C*, Three-dimensional CT skull reconstruction of subject 3541, aged 4 wk, showing complete synostosis of the metopic, sagittal, and coronal sutures. *D*, Preoperative radiographs of the hands and feet of subject 3734, aged 11 years. Note characteristic longitudinally split epiphyses at bases of several proximal phalanges, central polydactyly of the feet, and biphalangeal digits II of the hands and II and III of the feet.

2 combined, at chromosome 6p12.1-q12 (fig. 2A). The flanking heterozygous SNPs in family 1 were *rs7766181* and *rs10498828*, and the affected individual in family 2 was homozygous throughout this region.

The interval of homozygosity shared by the two families contained 24 annotated genes (Ensembl Genome Browser). Initially, we considered *BMP5* a candidate, because mutation of murine *Bmp5* causes a range of skeletal defects resulting in the *short ear* phenotype⁹; however, no mutations were found. We next analyzed *RAB23*; recessive nonsense mutations in the orthologous murine *Rab23* gene cause neural-tube defects, abnormal somites, polydactyly, and poorly developed eyes (*opb* [*open brain*] locus).^{10–12} With use of the primers listed in table 1, direct sequencing

of the seven exons and surrounding intronic regions of *RAB23* revealed an identical homozygous 434T→A transversion encoding an L145X nonsense mutation (fig. 3A) in the four affected individuals from families 1 and 2, as well as in a further sporadic case (subject 3734). These five subjects were all identically homozygous for 30 fully genotyped consecutive SNPs on the Affymetrix 50K array (from *rs10484709* to *rs1577630*) (fig. 2B), indicating that they were very likely to share a single ancestral mutation (see below).

To expand the mutation spectrum in *RAB23*, we ascertained 12 additional unpublished Carpenter syndrome cases unrelated by family history. Including the three families described above, the 15 independent families included 17 affected individuals from whom DNA was available; 6 cases arose from known consanguineous unions. The families originated from the United Kingdom (five), Brazil (five), The Netherlands (three), and Denmark and the United States (one each). The clinical features of these 17 cases, which represent the largest series of subjects with Carpenter syndrome to date, are presented in table 2. Craniosynostosis was present in all individuals, with the sutures affected with relative frequency sagittal>metopic>coronal>lambdoid. Abnormalities of the hands included postaxial polydactyly (9 of 17 cases), broad or bifid thumbs (6 of 17), cutaneous syndactyly (12 of 17), and absent middle phalanges (9 of 11). In the feet, preaxial or central polydactyly (16 of 17) and syndactyly (17 of 17) were nearly always present. High birth weight (9 of 9) and obesity (9 of 10) were prevalent. Other significant complications included umbilical hernia (8 of 17), congenital heart disease (3 of 17), deformities of the knees (4 of 14) or ankles (4 of 17), and cryptorchidism or hypoplastic testes in males (6 of 8). Brain imaging showed abnormalities in 7 of 10 subjects; 3 of 16 had hydrocephalus requiring insertion of a shunt. Significant learning disability was present in 6 of 13 individuals. The occurrence of an open neural-tube defect (family 2; subject 3624), although not previously described in Carpenter syndrome, is unlikely to be coincidental, because this is a cardinal feature of *Rab23* mutation in the mouse; the mother of subject 3624 had taken periconceptional folic acid supplements.

Pathogenic sequence variants were found in all individuals with the classic phenotype (table 3 and fig. 3A), showing that mutations of *RAB23* are the major cause of Carpenter syndrome. We identified five different mutations, all of which predict a loss of function. Four (E48fsX7, Y78fsX30, E137X, and L145X) of the five alleles are nonsense or frameshifting mutations that would generate truncated proteins. We identified a single missense mutation, C85R, encoding a nonconservative substitution from an uncharged to a charged amino acid; this residue is involved in β -sheet formation and is completely buried in the core of the protein (fig. 4),^{13,14} suggesting that this substitution would disrupt normal folding of *RAB23*. This mutation was present in individual 3961, who was a compound heterozygote for the C85R and L145X alleles; all

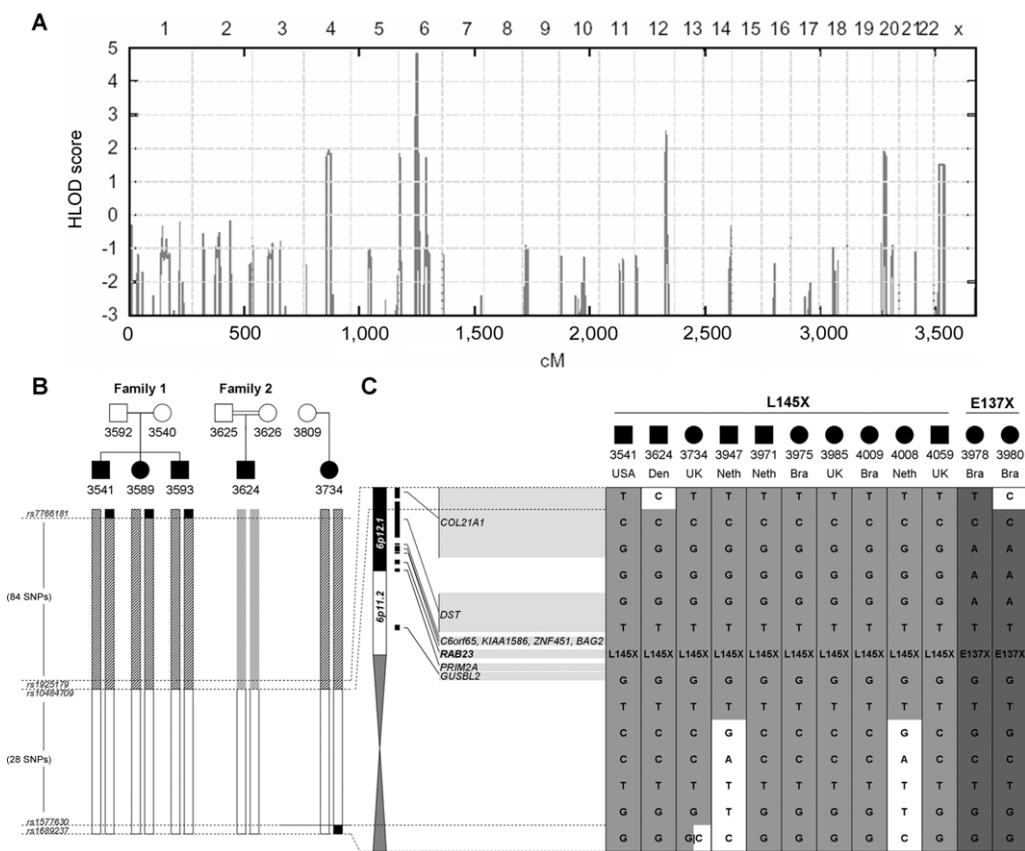


Figure 2. Linkage and haplotype mapping of Carpenter syndrome to chromosome 6p12.1. *A*, Genomewide HLOD scores from 50K microarray data for families 1 and 2 combined, with the assumption of a consanguineous loop (second-cousin parents) in family 1. HLOD scores are given along the Y-axis, relative to genomic position (cM) on the X-axis. Note the significant peak (HLOD 4.8) in the centromeric region of chromosome 6. *B*, Representation of 50K SNP haplotypes (vertical bars) for chromosomes of affected individuals in families 1 and 2 and an additional sporadic case (subject 3734), all of whom are homozygous for the 434T→A (L145X) mutation in *RAB23*. Distinct haplotypes are represented by different shaded bars. On the basis of homozygosity, the critical region on chromosome 6 is defined by heterozygosity for SNPs *rs7766181* (family 1) and *rs1689237* (subject 3734). Within this, a smaller region (white bars) is identical in all affected individuals for 30 consecutive SNPs, suggesting a common ancestral origin of the L145X mutation. *C*, Genotyping of 13 selected SNPs spanning this identical segment in 10 individuals homozygous for the L145X mutation and 2 individuals homozygous for E137X. At left, the position of these SNPs is shown in relation to *RAB23* and 8 additional genes within the 6p12.1-q11 region. Note that all patients with the L145X mutation share a common haplotype for seven consecutive SNPs; this is interrupted proximally in two Dutch patients, probably because of a shared recombination. From top to bottom, the genotyped SNPs are *rs1925179*, *rs2397214*, *rs9296842*, *rs1547625*, *rs6927258*, *rs6906792*, *rs3904827*, *rs6934928*, *rs1343391*, *rs1224703*, *rs1850417*, *rs2343013*, and *rs1689237*. Bra = Brazil; Den = Denmark; Neth = The Netherlands.

other affected individuals appeared homozygous for their particular mutation. When samples were unavailable from both parents but we had sufficient proband DNA, we excluded the possibility that one allele harbored a deletion (table 3) by multiplex ligation-dependent probe-amplification (MLPA) analysis using synthetic oligonucleotide probes to *RAB23* exons 1, 3, and 7 (MRC-Holland). All mutations were absent in ≥292 control chromosomes, as assessed by diagnostic restriction digests (fig. 3A and table 4).

The L145X mutation was apparently homozygous in 10 probands (3 each from the Netherlands and the United Kingdom, 2 from Brazil, and 1 each from the United States

and Denmark), 3 of whom had been shown by the Affymetrix SNP analysis to share a common haplotype around the mutation (fig. 2B). To check whether any of the other cases had arisen from an independent mutation, we genotyped them for a subset of 13 SNPs around *RAB23* (table 5). All 10 patients shared a common haplotype comprising 7 SNPs and spanning 2.2 Mb. This haplotype—which, according to HapMart (International HapMap Project), is present in only 11 of 120 Utah-CEPH chromosomes from HapMap¹⁶—was delimited by ancestral recombinations, distally in the Danish family and proximally in two Dutch families, and contains only eight genes in addition to *RAB23* (fig. 2C). These data indicate that a founder effect,

Table 1. Primers Used for PCR Amplification of *RAB23*

Primer	Primer Sequence (5'→3')		Product Size (bp)	Wave Temperature(s) (°C)
	Forward	Reverse		
RAB23_1	CTCCACCTGGCATTAGAC	AACAGCCCTTTTCAGACCTT	270	59
RAB23_2	CCACAGATTGAGAGGGAAGA	AGTTGCCACACCTCGAAATC	333	56.4
RAB23_3	TTACCAAAAACATTTTCCTTACA	GCCAAAATAATATGCCAAA	188	54
RAB23_4	TGTTAATGTAATACCTTGATTGATG	TATAGAATACTGTCCCTCTTCCC	250	56.5 and 58.5
RAB23_5	AAACAAGCTATCAGAAGGCACC	CAACACAATTTAAAAGCGCA	207	54.5
RAB23_6	ATCATTGACCTGGTTCTGGG	TCACTTTAAATCACATTTCTGAAAGA	228	55
RAB23_7	TAACCTCAGGCGTGTCAGTGG	ATGACAGCTGGATGGGTTTC	256	57

NOTE.—DNA was obtained from whole-blood samples by phenol-chloroform extraction and was amplified in a total volume of 25 μ l containing 15 mM TrisHCl (pH 8.0), 50 mM KCl, 2.5 mM MgCl₂, 100 μ M each deoxy-nucleoside triphosphate, 0.5 μ M primers, and 0.75 units of Amplitaq Gold polymerase (Applied Biosystems). All PCRs were performed using an annealing temperature of 60°C. Cycling conditions consisted of an 8-min denaturation step at 94°C, followed by 35 cycles at 94°C for 30 s, at 60°C for 30 s, and at 72°C for 60 s, with a final extension at 72°C for 10 min.

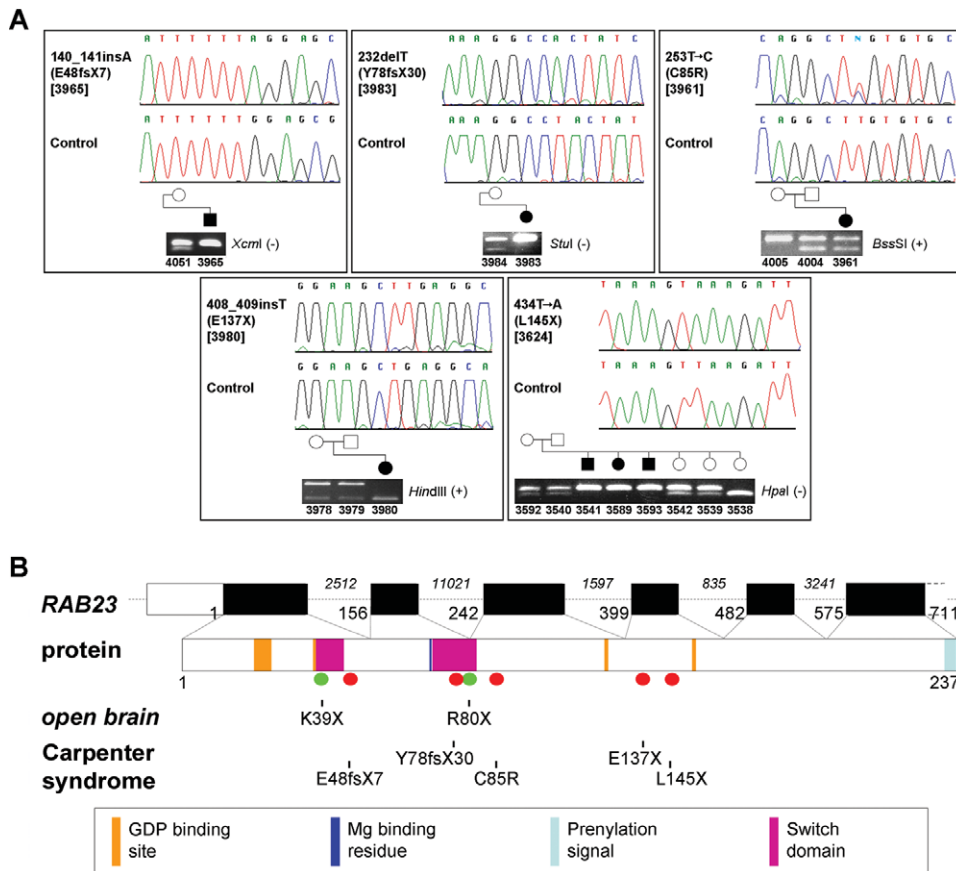


Figure 3. *RAB23* mutations in Carpenter syndrome. A, Sequence chromatograms and confirmatory restriction digests for the five pathogenic mutations identified. Note that patient 3961 is a compound heterozygote for the C85R and L145X mutations. **B, top,** The exon/intron organization of *RAB23*, with the coding part of the cDNA (GenBank [accession number NM_183227.1]; Ensembl Genome Browser [reference OTTHUMG00000014918]) in black and the UTRs in white (alternatively spliced 5' noncoding exons omitted). Plain numbering refers to the first nucleotide of each exon, starting from the initiation codon, and italic numbering indicates the length of introns. **Bottom,** Functional domains in the 237-aa protein,^{13,14,17} color coded, with the location of human mutations causing Carpenter syndrome and those found in *open brain* mice¹² indicated by red and green dots, respectively. GDP=guanosine diphosphate.

Table 2. Clinical Features of Patients with Mutations in *RAB23*

The table is available in its entirety in the online edition of *The American Journal of Human Genetics*.

rather than a recurrent mutation, underlies Carpenter syndrome in patients of northern European descent and does not support the possibility that the L145X mutation has particular functional consequences (see below). Two patients from eastern Brazil both appeared homozygous for the E137X mutation, which resides on a shared haplotype spanning at least 5.8 Mb (fig. 2C). The E48fsX7 and Y78fsX30 mutations were each found in one patient only.

To explore whether *RAB23* mutations play a more general pathological role either in craniosynostosis or in limb malformations, we screened respective patient panels by a combination of Wave denaturing high-performance liquid chromatography (Transgenomic) and diagnostic restriction digests for mutations identified in Carpenter syndrome. DNA from 256 patients with craniosynostosis (negative for the common mutations in the *FGFR1*, *FGFR2*, *FGFR3*, and *TWIST1* genes),⁶ 202 patients with limb malformations requiring plastic surgery, and 163 control individuals was analyzed using the assays detailed in tables 1, 4, and 6. None of the Carpenter syndrome mutations (table 3) were identified in any of these cohorts. Although six novel alleles—including an amino acid substitution, an amino acid deletion, and a nonsense mutation (all in the heterozygous state)—were found in the patient groups (table 6), none appeared related to the clinical phenotype. An additional common nonsynonymous SNP c.619G→A (p.G207S; *rs1040461*) was present, for which all three genotypes were identified in unaffected individuals in the HapMap panel.¹⁶ These results show that *RAB23* mutations

do not frequently contribute either to craniosynostosis or to limb malformations.

Rab23, first isolated from the mouse in 1994,¹⁷ belongs to the RAB family of >60 small guanosine triphosphatases (GTPases) that regulate intracellular trafficking of membrane-associated proteins^{13–15}; other family members for which germline mutations cause human disorders are *RAB7* (Charcot-Marie-Tooth disease type 2B, dominant inheritance [MIM #600882])¹⁸ and *RAB27A* (Griscelli syndrome type 2, recessive inheritance [MIM #607624]).¹⁹ Our finding of *RAB23* mutations in Carpenter syndrome is unexpected, because similar nonsense mutations of the orthologous murine *Rab23* gene (encoding K39X and R80X) in *opb* mice cause recessive embryonic lethality with exencephaly.^{10–12} It is unlikely that the human *RAB23* mutations represent partial loss-of-function alleles of lesser severity than do the murine ones, for two reasons. First, prenylation at a consensus site in the C-terminus of RAB proteins by RAB geranylgeranyl transferase is essential for their correct membrane targeting,¹⁵ predicting that all truncating mutations should result in complete loss of function. Second, two of the human truncating mutations (E48fsX7 and Y78fsX30) occur upstream of the *opb* mutation R80X (fig. 3B),¹² yet neural-tube defects were absent in the affected individuals. Consistent with this, we did not find any clear genotype-phenotype correlation for the human mutations, although the fetus 3965, with the most N-terminal truncation (E48fsX7), was the only subject terminated antenatally and might represent a more severe phenotype (table 2).

The original identification of *Rab23* mutations in *opb* mice was driven by genetic studies to identify modifiers of hedgehog (HH) signaling in the neural tube. In mammals, there are three paralogous HH genes—*Shh*, *Ihh*, and

Table 3. *RAB23* Mutations in Patients with Carpenter Syndrome

Subject	Sex	Parental Consanguinity	Country of Origin	Ethnicity	Sample(s) Analyzed ^a	Mutation at Allele			
						Maternal		Paternal	
						DNA	Protein	DNA	Protein
3965	M	—	United Kingdom	White	C and M	140_141insA	E48fsX7	140_141insA	E48fsX7
3983	F	1st cousin	Brazil	African/white	C and M	232delT	Y78fsX30	Same ^b	—
3961	F	—	United Kingdom	White	C, M, and F	434T→A	L145X	253T→C	C85R
3978	F	—	Brazil	African/white	C and M	408_409insT	E137X	408_409insT	E137X
3980	F	1st cousin once removed	Brazil	White	C, M, and F	408_409insT	E137X	Same	—
3541 (Family 1)	M	—	United States	White	C, M, and F	434T→A	L145X	434T→A	L145X
3589 (Family 1)	F	—	United States	White	C, M, and F	434T→A	L145X	434T→A	L145X
3593 (Family 1)	M	—	United States	White	C, M, and F	434T→A	L145X	434T→A	L145X
3624 (Family 2)	M	1st cousin	Denmark	White	C, M, and F	434T→A	L145X	Same	—
3734	F	—	United Kingdom	White	C and M	434T→A	L145X	434T→A ^b	L145X
3947	M	—	Netherlands	White	C, M, and F	434T→A	L145X	434T→A	L145X
3971	M	1st cousin	Netherlands	White	C, M, and F	434T→A	L145X	Same	—
3975	M	1st cousin	Brazil	White	C, M, and F	434T→A	L145X	Same	—
3985	F	—	United Kingdom	White	C, M, and F	434T→A	L145X	434T→A	L145X
4008	F	—	Netherlands	White	C	434T→A	L145X	434T→A	L145X
4009	M	1st cousin	Brazil	African	C, M, and F	434T→A	L145X	Same	—
4059	M	—	United Kingdom	White	C	434T→A	L145X	434T→A	L145X

NOTE.—Nucleotide numbering of *RAB23* cDNA is based on GenBank sequence NM_183227.1 but starts from the first base of the initiation codon. For cases in which the two parental alleles are very unlikely to be independent (due to known consanguinity), the paternal allele is denoted “Same.”

^a C = child; M = mother; F = father.

^b Complete deletion of one allele was not formally excluded by MLPA analysis.

Table 5. Primers and Restriction Enzymes Used for Haplotype Analysis

Primer	Primer Sequence (5'→3')	Product Size (bp)	Assay ^a
rs1925179F	GGCAGCTTTCTCTGACTG	188	<i>Hpy188I</i>
rs1925179R	TTACATTTCAAAGGGGTGGC		
rs2397214F	GGCCTGTGATTTGAGTGGTT	165	<i>MnII</i>
rs2397214R	TCTCTGTGACCAGATGCCA		
rs9296842F	CTGAAGTTGCATTCCTGCCA	165	<i>BtsCI</i>
rs9296842R	AAATTAATAATCAGTGTCTGCCA		
rs1547625Fseq	CCTGGCCTCATCTACCATA	154	Seq
rs1547625Rseq	TGCCTGAGAAAAATGAGGCT		
rs6927258F	TTCTGATCATGATGATGCCA	218	<i>MboI</i>
rs6927258R	GGGCTTGGCATCTCTGAGTA		
rs6906792Fseq	CAGAACTTGGCAACAAAATG	182	Seq
rs6906792Rseq	TTCTGGGAATTTAAAAGGTAGCA		
rs3904827F	ACTGCATACCCTTACAAA	275	<i>Tsp509I</i>
rs3904827R	TCCAGACAAAACAAAGGCTGA		
rs6934928F	AAGTGGCTTATTTCTCCAAGA	180	<i>RsaI</i>
rs6934928R	GCCCAAATCCATGTAATCTCT		
rs1343391Fseq	AAGGAGAGGGAGAGACCGAG	187	Seq
rs1343391Rseq	AGCACATGATATGCCACTT		
rs1224703F	AATAGGGCAGAAGGGTGCTC	195	<i>Tsp509I</i>
rs1224703R	ACCCACAAAAGAGACGTGAG		
rs1850417F	CTTTAACTCCATTTTAAGGGACAG	190	<i>EarI</i>
rs1850417R	AACAAGCTTGGAGAAGCAAA		
rs2343013F	TGTGTTCCCAACTGCTGAA	221	<i>MwoI</i>
rs2343013R	CATCTCCCCGGTTAAACTT		
rs1689237Fseq	TGAGGGATCTGGGATGCTAC	157	Seq
rs1689237Rseq	TTTAGCTCTCACTGCATGGC		

NOTE.—PCRs were performed using the same conditions as described in table 1.

^a Seq = analysis by DNA sequencing.

Dhh—encoding the sonic, Indian, and desert HH proteins, respectively.^{20,21} The *opb* locus was initially described in a sporadically occurring mouse mutant with exencephaly¹⁰ (a variably expressed phenotype observed on both C57Bl/6 and C3H backgrounds).^{10,11} Subsequently, a second allele was isolated in an ethylnitrosourea mutagenesis screen for recessive embryonic lethal mutations²²; nonsense mutations of *Rab23* were demonstrated in both strains.¹² Homozygosity for these *opb* mutations rescues many of the morphological defects in *Shh*^{-/-} mice, with *Shh/opb* double-mutant mice largely resembling *opb* single mutants,

indicating that the *Rab23* mutations bypass the requirement for *Shh*.¹² In the neural tube, mutation of *Shh* has opposite consequences to mutation of *Rab23*, causing loss (*Shh*) and expansion (*Rab23*) of ventral markers; Patched1, a transcriptional target of Shh signaling, is activated in *opb* mice, showing that Rab23 is a negative regulator of HH signaling.^{11,12} Genetic analysis of epistatic relationships shows that Rab23 acts downstream of the key HH signaling intermediate Smoothed but upstream of both the effector transcription factors Gli2 and Gli3²³ and the intraflagellar transport proteins (such as those encoded by *Ift88/polaris* and *Ift172/wim*), required for their capacitation.²⁴ As such, *Rab23* is one of a number of genes (including *iguana*, *talpid*³, *Fkbp8*, and Ift family members) implicated in the regulation of Gli transcription-factor processing specifically in vertebrates^{21,25} and is the first of these implicated in a human disorder. Rab23 localizes to membranes^{26,27} and is expressed at multiple sites in the mouse, including embryonic neural tube, limb bud, branchial arches, tooth and palate,^{12,28,29} and adult brain²⁷; however, its precise membrane-transport activity has not been defined.

Given the evidence that Rab23 regulates the HH pathway, it is not surprising that some aspects of the phenotype of Carpenter syndrome resemble other human disorders associated with disturbed HH signaling. Most notably, the combination of postaxial polysyndactyly of the hands and preaxial polysyndactyly of the feet is very similar to the pattern that occurs in Greig syndrome (MIM #175700), which is due to haploinsufficiency of GLI3,³⁰ and is consistent with the observed reduction in the proportion of Gli3 repressor in *Rab23*-mutant embryos.²³ The brachydactyly present in Carpenter syndrome, characterized by hypoplasia or absence of the middle phalanges, resembles brachydactyly type A1, which is caused by heterozygous missense mutations in *IHH* that appear to cluster on one surface of the protein and disrupt phalangeal patterning by an unknown mechanism.³¹ However, the viability of the human *RAB23* homozygous mutations in Carpenter syndrome uncovers several phenotypes (table 2), not previously observed in the lethal *opb* mouse mu-

Table 6. RAB23 Variants Identified in Patients with Craniosynostosis and Limb Malformations

dbSNP Accession Number	Nucleotide	Amino Acid	Exon (Intron)	No. of Heterozygotes			Present in Unaffected Parent ^a	Restriction Digest
				With Craniosynostosis (N = 256)	With Limb Malformation (N = 202)	Controls (N = 163)		
ss69357975	c.1-49C→G	—	(1)	2	0	0	NT	<i>Hpy188III</i> (—)
ss69357972	c.39_41del	p.V13del	2	1	0	0	NA	<i>XcmI</i> (—)
ss69357968	c.119A→G	p.K40R	2	0	0	1	—	NT
ss69357974	c.155+44C→A	—	(2)	0	0	1	—	NT
ss69357973	c.242-15_-12del	—	(3)	0	1	0	NA	NT
ss69357971	c.247C→T	p.Q83X	4	1	0	0	NA	<i>BfaI</i> (+)
ss69357970	c.301T→G	p.S101A	4	5	2	2	2 (5 NA)	<i>MwoI</i> (+)
ss69357969	c.574+28G→A	—	(6)	0	1	1	NA	NT

NOTE.—NT = not tested.

^a NA = one or both parents unavailable for testing.

tants,^{10–12,22} that are not well recognized features of perturbed HH signaling.²⁰ Particularly interesting are the craniosynostosis and tendency to postnatal obesity, which may provide new clues for dissecting the pathophysiology of these phenotypes.

Relatively little is known about the role of HH signaling in the cranial sutures. In mice, *Shh* is expressed in the osteogenic fronts of the parietal bones and sagittal sutures only at a relatively late stage of suture development (embryonic day 17),³² and *Shh*^{-/-} mice die too early to assess the developmental contribution to the cranial sutures. Although endochondral ossification is characteristically deficient in *Ihh*^{-/-} mice, membranous ossification of the skull vault is maintained³³; however, there are no published data on the expression pattern of *Ihh* in the sutures. Our work should stimulate efforts to identify the active HH ligand(s) and to explore the extent to which the well-documented developmental relationship among HH signaling, twist, and FGF receptors in the limbs³⁴ is recapitulated in the cranial suture. There is a potential pathophysiological link with Antley Bixler syndrome (MIM #207410), another recessively inherited craniosynostosis caused by mutations in *P450 oxidoreductase (POR)*.³⁵ POR is the single flavoprotein involved in electron transfer to all cytochrome P450 enzymes, including several involved in cholesterol biosynthesis, defects of which disrupt HH signaling.³⁶

Although postnatal obesity (which has a central distribution) is practically universal in subjects with Carpenter syndrome, its neuroendocrinological and biochemical bases are not known. Obesity has not been described elsewhere in mammalian disorders of HH signaling²⁰ and was not observed in *opb* mice, probably because of embryonic lethality. Pharmacological approaches have previously suggested that HH signaling may regulate adipogenesis, but the results have been conflicting as to whether this effect was inhibitory or stimulatory.³⁷ The association of *RAB23* mutations with obesity may provide new insight into the role of HH signaling in the control of fat metabolism. Alternatively, this phenotype may reflect either the regulation of *RAB23* itself (possibly by bone morphogenetic proteins)¹² or downstream HH-independent processes. The possible interaction of *RAB23* with cilia²¹ suggests an overlap with the Bardet-Biedl syndromes, which are ciliopathies that also feature obesity and polydactyly.³⁸

Acknowledgments

We thank all the families for their participation in this study; S. Balci and A. Richieri-Costa for referring patient samples; C. Becker (Nürnberg laboratory) for expert technical assistance in providing the SNP genotype data from Affymetrix microarrays; other members of the Wilkie laboratory for their support, especially D. Furniss for access to samples from patients with limb malformations and I. Taylor for DNA extraction; K. Clark for DNA sequencing; and J. Eggenschwiler and B. St-Jacques for discussions. This work was funded by the E. P. Abraham Cephalosporin Fund (support to D.J.), German Federal Ministry of Sciences and Education

through the National Genome Research Network grant 01GR0416 (to P.N.), and the Wellcome Trust (support to A.O.M.W.).

Web Resources

Accession numbers and URLs for data presented herein are as follows:

dbSNP, <http://www.ncbi.nlm.nih.gov/SNP/> (for SNPs, including *rs1040461*, *rs1925179*, *rs2397214*, *rs9296842*, *rs1547625*, *rs6927258*, *rs6906792*, *rs3904827*, *rs6934928*, *rs1343391*, *rs1224703*, *rs1850417*, *rs2343013*, and *rs1689237*)

Ensembl Genome Browser, <http://www.ensembl.org/> (for *RAB23* [reference OTTHUMG00000014918])

GenBank, <http://www.ncbi.nlm.nih.gov/Genbank/> (for human *RAB23* cDNA reference sequence [accession number NM_183227.1])

International HapMap Project, <http://hapmart.hapmap.org/BioMart/martview> (for HapMart)

MRC-Holland, <http://www.mrc-holland.com/pages/indexpage.html> (for information on MLPA reagents and methods)

Online Mendelian Inheritance in Man (OMIM), <http://www.ncbi.nlm.nih.gov/Omim/> (for Carpenter syndrome, Charcot-Marie-Tooth disease type 2B, Griscelli syndrome type 2, Greig syndrome, and Antley Bixler syndrome)

Protein Data Bank, <http://www.rcsb.org/pdb/home/home.do> (for *RAB23* structure [number 1Z22] and Protein Workshop)

References

1. Carpenter G (1901) Two sisters showing malformations of the skull and other congenital abnormalities. *Rep Soc Study Dis Child Lond* 1:110–118
2. Carpenter G (1909) Case of acrocephaly, with other congenital malformations. *Proc Roy Soc Med* 2:45–53
3. Temtamy SA (1966) Carpenter's syndrome: acrocephalopolysyndactyly. *J Pediatr* 69:111–120
4. Robinson LK, James HE, Mubarak SJ, Allen EJ, Jones KL (1985) Carpenter syndrome: natural history and clinical spectrum. *Am J Med Genet* 20:461–469
5. Cohen DM, Green JG, Miller J, Gorlin RJ, Reed JA (1987) Acrocephalopolysyndactyly type II—Carpenter syndrome: clinical spectrum and an attempt at unification with Goodman and Summit syndromes. *Am J Med Genet* 28:311–324
6. Morriss-Kay GM, Wilkie AOM (2005) Growth of the normal skull vault and its alteration in craniosynostosis: insights from human genetics and experimental studies. *J Anat* 207: 637–653
7. Perlyn CA, Marsh JL (2007) Craniofacial dysmorphology of Carpenter syndrome: lessons from three affected siblings. *Plast Reconstr Surg* (in press)
8. Dietter J, Mattheisen M, Fürst R, Rüschemdorf F, Wienker TF, Strauch K (2007) Linkage analysis using sex-specific recombination fractions with GENEHUNTER-MODSCORE. *Bioinformatics* 23:64–70
9. King JA, Marker PC, Seung KJ, Kingsley DM (1994) BMP5 and the molecular, skeletal, and soft-tissue alterations in *short ear* mice. *Dev Biol* 166:112–122
10. Günther T, Struwe M, Aguzzi A, Schughart K (1994) *open brain*, A new mouse mutant with severe neural tube defects, shows altered gene expression patterns in the developing spinal cord. *Development* 120:3119–3130
11. Eggenschwiler JT, Anderson KV (2000) Dorsal and lateral fates

- in the mouse neural tube require the cell-autonomous activity of the *open brain* gene. *Dev Biol* 227:648–660
12. Eggenchwiler JT, Espinoza E, Anderson KV (2001) Rab23 is an essential negative regulator of the mouse sonic hedgehog signalling pathway. *Nature* 412:194–198
 13. Pereira-Leal JB, Seabra MC (2000) The mammalian Rab family of small GTPases: definition of family and subfamily sequence motifs suggests a mechanism for functional specificity in the Ras superfamily. *J Mol Biol* 301:1077–1087
 14. Eathiraj S, Pan X, Ritacco C, Lambright DG (2005) Structural basis of family-wide Rab GTPase recognition by rabenosyn-5. *Nature* 436:415–419
 15. Pereira-Leal JB, Seabra MC (2001) Evolution of the Rab family of small GTP-binding proteins. *J Mol Biol* 313:889–901
 16. The International HapMap Consortium (2005) A haplotype map of the human genome. *Nature* 437:1299–1320
 17. Olkkonen VM, Peterson JR, Dupree P, Lütcke A, Zerial M, Simons K (1994) Isolation of a mouse cDNA encoding Rab23, a small novel GTPase expressed predominantly in brain. *Gene* 138:207–211
 18. Verhoeven K, De Jonghe P, Coen K, Verpoorten N, Auer-Grumbach M, Kwon JM, FitzPatrick D, Schmedding E, De Vriendt E, Jacobs A, et al (2003) Mutations in the small GTPase late endosomal protein RAB7 cause Charcot-Marie-Tooth type 2B neuropathy. *Am J Hum Genet* 72:722–727
 19. Ménasché G, Pastural E, Feldmann J, Certain S, Ersoy F, Dupuis S, Wulffraat N, Bianchi D, Fischer A, Le Deist F, et al (2000) Mutations in *RAB27A* cause Griscelli syndrome associated with haemophagocytic syndrome. *Nat Genet* 25:173–176
 20. Nieuwenhuis E, Hui C-c (2005) Hedgehog signaling and congenital malformations. *Clin Genet* 67:193–208
 21. Huangfu D, Anderson KV (2006) Signaling from Smo to Ci/Gli: conservation and divergence of Hedgehog pathways from *Drosophila* to vertebrates. *Development* 133:3–14
 22. Kasarskis A, Manova K, Anderson KV (1998) A phenotype-based screen for embryonic lethal mutations in the mouse. *Proc Natl Acad Sci USA* 95:7485–7490
 23. Eggenchwiler JT, Bulgakov OV, Qin J, Li T, Anderson KV (2006) Mouse Rab23 regulates Hedgehog signaling from smoothed to Gli proteins. *Dev Biol* 290:1–12
 24. Huangfu D, Liu A, Rakeman AS, Murcia NS, Niswander L, Anderson KV (2003) Hedgehog signalling in the mouse requires intraflagellar transport proteins. *Nature* 426:83–87
 25. Davey MG, Paton IR, Yin Y, Schmidt M, Bangs FK, Morrice DR, Gordon Smith T, Buxton P, Stamatakis D, Tanaka M, et al (2006) The chicken *talpid3* gene encodes a novel protein essential for Hedgehog signaling. *Genes Dev* 20:1365–1377
 26. Evans TM, Ferguson C, Wainwright BJ, Parton RG, Wicking C (2003) Rab23, a negative regulator of hedgehog signaling, localizes to plasma membrane and the endocytic pathway. *Traffic* 4:869–884
 27. Guo AC, Wang T, Ng EL, Aulia S, Chong KH, Teng FYH, Wang Y, Tang BL (2006) *Open brain* gene product Rab23: expression pattern in the adult mouse brain and functional characterization. *J Neurosci Res* 83:1118–1127
 28. Miletich I, Cobourne MT, Abdeen M, Sharpe PT (2005) Expression of the Hedgehog antagonists *Rab23* and *Slimb/βTrCP* during mouse tooth development. *Arch Oral Biol* 50:147–151
 29. Rice R, Connor E, Rice DPC (2006) Expression patterns of Hedgehog signalling pathway members during mouse palate development. *Gene Expr Patterns* 6:206–212
 30. Biesecker LG (2004) GLI3 and the Pallister-Hall and Greig cephalopolysyndactyly syndromes. In: Epstein CJ, Erickson RP, Wynshaw-Boris A (eds) *Inborn errors of development*. Oxford University Press, Oxford, United Kingdom, pp 257–264
 31. Hellemans J, Coucke PJ, Giedion A, De Paepe A, Kramer P, Beemer F, Mortier GR (2003) Homozygous mutations in *IHH* cause acrocapitofemoral dysplasia, an autosomal recessive disorder with cone-shaped epiphyses in hands and hips. *Am J Hum Genet* 72:1040–1046
 32. Kim H-J, Rice DPC, Kettunen PJ, Thesleff I (1998) FGF-, BMP- and Shh-mediated signalling pathways in the regulation of cranial suture morphogenesis and calvarial bone development. *Development* 125:1241–1251
 33. St-Jacques B, Hammerschmidt M, McMahon AP (1999) Indian hedgehog signaling regulates proliferation and differentiation of chondrocytes and is essential for bone formation. *Genes Dev* 13:2072–2086
 34. O'Rourke MP, Soo K, Behringer RR, Hui C-c, Tam PP (2002) *Twist* plays an essential role in FGF and SHH signal transduction during mouse limb development. *Dev Biol* 248:143–156
 35. Huang N, Pandey AV, Agrawal V, Reardon W, Lapunzina PD, Mowat D, Jabs EW, Van Vliet G, Sack J, Flück CE, et al (2005) Diversity and function of mutations in P450 oxidoreductase in patients with Antley-Bixler syndrome and disordered steroidogenesis. *Am J Hum Genet* 76:729–749
 36. Cooper MK, Wassif CA, Krakowiak PA, Taipale J, Gong R, Kelley RI, Porter FD, Beachy PA (2003) A defective response to Hedgehog signaling in disorders of cholesterol biosynthesis. *Nat Genet* 33:508–513
 37. Rosen ED (2006) New drugs from fat bugs? *Cell Metab* 3:1–2
 38. Badano JL, Mitsuma N, Beales PL, Katsanis K (2006) The ciliopathies: an emerging class of human genetic disorders. *Annu Rev Genomics Hum Genet* 7:125–148